Renewable Energy 115 (2018) 423–432

Contents lists available at ScienceDirect

Renewable Energy

journal homepage: www.elsevier.com/locate/renene

Integrating desalination with concentrating solar thermal power: A Namibian case study

J.E. Hoffmann [a, *], E.P. Dall [b]

[a] Department of Mechanical & Mechatronic Engineering, Stellenbosch University, South Africa
[b] NamPower, Power Systems Development Business Unit, South Africa

ARTICLE INFO

Article history:
Received 27 May 2017
Received in revised form
4 August 2017
Accepted 23 August 2017
Available online 30 August 2017

Keywords:
Cogeneration of water and electricity
Concentrating solar power
Central receiver
Desalination
Multi-effect distillation
Namibia

ABSTRACT

This paper reports on a feasibility study into the integration of a multi-effect distillation plant with a central receiver plant to generate electricity for the Namibian grid, and fresh water for the community and mining operations at Arandis. Arandis receives on average 2528 kWh/m^2/year of solar irradiation, is only 48 km from the coast and 580 m above sea level, making it attractive for a cogeneration plant. Desalination is energy intensive, but the required energy is freely available from the waste heat rejected at the condenser of a Rankine cycle. In this study, high level thermodynamic models of a multi-effect distillation and central receiver plant were developed to better understand the economics of such a cogeneration plant. Results indicate that a 100 MW$_e$ central receiver plant combined with a multi-effect distillation plant, is capable of servicing the current water demand in the region. Despite the high capital costs of central receiver plant, as well as pumping seawater inland, the plant is economically viable within the proposed tariff structure for renewable energy in Namibia, and existing water tariffs. Profit parity between a cogeneration plant and a stand-alone, dry-cooled central receiver plant is reached for top brine temperatures above 65 °C. Under these conditions, water sales would subsidize electricity production. However, it is not price competitive with a grid-powered reverse osmosis plant on the coast. The most significant barriers in making cogeneration plant competitive against more conventional desalination methods such as reverse osmosis are the high capital cost of the cogeneration plant, and pumping seawater inland.

1. Introduction

Namibia is one of the most water stressed countries in sub-Saharan Africa, but it is also blessed with one of the highest solar resources in the world. It is a sparsely populated country, with most people living in the wetter north. South and central Namibia relies largely on underground water resources for potable water, mining and agricultural activities. These aquifers are rapidly depleted, and in coastal regions, seepage from seawater put this resource at risk of salinization. Recharge is sporadic, forcing authorities to cap annual extraction from these aquifers. The United Nations [1] classified Namibia's water resources as currently stressed, and becoming vulnerable by 2025. It is expected that climate change will impact central Namibia severely over the next century, resulting in higher ambient air temperatures, and lower and more erratic rainfall [2]. Water scarcity might put future economic development in the mineral-rich central coastal region at risk.

Mining is the largest sector of the Namibian economy (11.5% of GDP), and is responsible for more than 50% of its foreign income [3]. Uranium mining is concentrated around Arandis, a town in the Erongo region, 48 km from the coast. Uranium mining is water intensive, and the demand for water will increase with the opening of the Husab mine in 2017. The increase in demand would place severe stress on the Omdel aquifer that supplies the Rössing uranium mine, and has prompted the construction of the first large desalination plant. The Trekkopje desalination plant at Swakopmund is a reverse osmosis plant with a capacity of 20 $\times$ 10^6 m^3/year, and will supply fresh water to the mines, Arandis and the coastal communities of Walvis Bay and Swakopmund. It has also increased the unit cost of water by almost 400% [4].

South, central and western Namibia has some of the highest solar resources in the world, as shown in Fig. 1. NamPower intends to tap into this resource [5], and has selected Arandis as the preferred site for a 50–300 MW$_e$ mixed solar park, comprising of a

* Corresponding author.
E-mail address: hoffmaj@sun.ac.za (J.E. Hoffmann).

http://dx.doi.org/10.1016/j.renene.2017.08.060
0960-1481/

Nomenclature

A	area, m^2
C_p	specific heat, J/kg °C
D	diameter, m
H	height, m
h	convective heat transfer coefficient, W/m^2 °C enthalpy, J/kg
L	length, m
$\dot{m}$	mass flow rate, kg/s
N	number of effects
NTU	number of transfer units
Q	heat, W
T	temperature, °C or K
U	overall heat transfer coefficient
V	velocity, m/s
X	Salinity, g/kg

Greek symbols

α	absorptivity
Δ	difference
ε	emissivity effectiveness
η	efficiency
σ	Stefan-Boltzman constant

Subscripts

a	air
a,g	air at ground level
b	brine
be	brine exit
bi	brine inlet
bo	brine out
D	diameter
d	distillate
d,b	distilate vapour formed due to boiling
d,f	distilate vapour formed due to flashing
dl	distilate in liquid phase
e	evaporator
f	feedwater
fi	feedwater in
fo	feedwater outlet
gd	distillate in gaseous phase
in	inlet
l	length
ph	preheater
rec	receiver
ref	reference
s	steam
si	steam inlet
so	steam out
t	tower
w	wall

concentrated solar thermal plant with thermal energy storage, and a photo-voltaic plant [6]. The annual direct normal irradiation (DNI) for Arandis is 2528 kW/m^2/year. Although this is not as high as the DNI's recorded in southern Namibia, the necessary electricity distribution network, road and rail infrastructure, its close proximity to the Walvis Bay harbour, local electricity demand, etc. makes Arandis an attractive location. The Namibian Electricity Control Board is contemplating a renewable energy feed-in tariff, comprising of a base tariff of N$1.90/kWh and a 50% share of the green energy credit, to independent power producers [7]. The National Renewable Energy Policy for Namibia is currently in draft form.

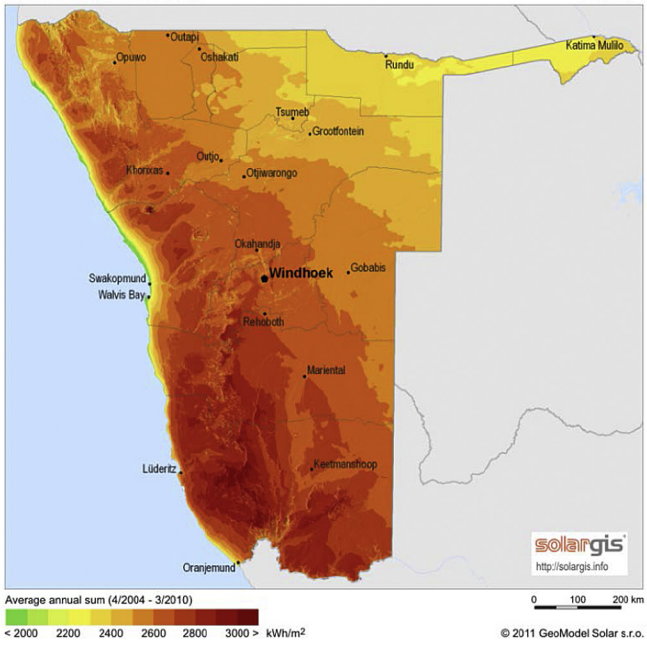

Fig. 1. DNI map for Namibia.

Namibia's power consumption is relatively low, with peak demand reaching 656 MW [8]. Most of it is supplied by the Ruacana Hydropower Scheme (340 MW) and the Van Eck coal fired power station. Output by Ruacana is restricted by seasonal rainfall, resulting in Namibia importing up to 60% of its annual electricity demand from the Southern African Power Pool. To accommodate future economic growth, and becoming energy independent, Namibia intends to expand its power production, mainly through renewable energy [9]. A target of 70% of its energy demand to be met by renewable energy by 2030 was set in the Namibian government's Vision 2030 document [10].

Thermal distillation of seawater was initially introduced to supplement fresh water supplies on ocean-bound ships during extended voyages [11]. Middle Eastern countries were the first to utilize desalination on a large scale for the use of municipal drinking water [12]. Reverse osmosis is currently the preferred technology, but its performance is sensitive to feed-water turbidity, salinity and temperature [13], necessitating pre-treatment of feed-water. Thermal distillation involves heating and evaporating seawater, and condensing the vapour. Multi-stage flash distillation relies on heating the seawater to its boiling point, and then flashing liquid to vapour by lowering pressure between subsequent stages. It accounts for more than 50% of the total installed desalination plants world-wide [14]. Seawater inlet temperatures to the first stage typically exceed 100 °C [15]. Multi-effect distillation (MED) relies mostly on boiling; the temperature and pressure are lowered between subsequent stages to allow boiling at a lower temperature,

using the latent heat of condensation from the previous stage as heat source. Seawater inlet temperatures are usually kept below 70 °C to prevent scaling. Vertically stacked multi-effect distillation plant is considered most suitable for solar heating, as it operates stably through large, rapid thermal input swings [16].

There is a synergy between concentrated solar power (CSP) generation and desalination of seawater [17]. The desalination plant effectively replaces the condenser in the Rankine cycle, whilst the Rankine cycle in turn provides a ready source of low grade heat for desalination. However, DNI at the coast is generally low, and the CSP plant should be build further inland. As a result, pumping whole seawater inland has a significant impact on the levelized cost of desalinated seawater.

Cogeneration of electricity and desalinated water is a relatively new concept, with commercial plants operating in Libya and Yemen [18] and a small pilot plant in Cyprus [19]. Techno-economic studies on various configurations of CSP and/or photovoltaic plant combined with desalination and/or reverse osmosis plants were done amongst others by Refs. [17,20–23]. Servert el al [17] concluded that CSP with multi-effect distillation is technically feasible, but more expensive than grid-powered reverse osmosis to supply fresh water to mining communities in the Atacama Desert in Chile. If no grid power is available, CSP with desalination offers a lower cost option to photo-voltaic driven reverse osmosis, mainly due to the higher capacity factors that can be realized from CSP plant with thermal energy storage. Their study was based on a location 100 km from the coast at an elevation of 2200 m above sea level.

This paper adds to the techno-economic studies on cogeneration of electricity and desalinated water, specifically for a site at Arandis, Namibia. The site has already been selected by NamPower for their solar park, as it is expected to have the lowest cost of generation [24]. Furthermore, it is relatively close to the sea, not too high above sea level, and there is an existing and pressing demand for fresh water. We have assumed a 100 MW_e nett power tower plant with molten salt as heat transfer fluid, using a two-tank thermal energy storage facility. The Namibian Energy Institute [25] predicts a slight economic advantage for a central receiver plant compared to a parabolic trough plant of the same rating. Plant parameters such as storage size, solar multiple, condenser temperature and number of effects in the distillation plant were subject to optimization. Results were compared to a status quo situation, comprising of grid-powered reverse osmosis (the Trekkopje desalination plant at Swakopmund) and a planned stand-alone CSP plant with a direct air-cooled condenser. This study was motivated by Rössing Uranium planning an additional desalination plant [4].

2. Model description

2.1. Direct normal irradiation

Satellite based hourly averaged DNI data for Arandis, Namibia (22°, 25′ South, 14°, 58′ East) for the year spanning from 1 November 2014–31 October 2015 were obtained directly from GeoSun Africa. The nominal design point for the CSP plant was solar noon on the autumn equinox, yielding a direct normal irradiation of 827 W/m^2 and an ambient temperature of 34.9 °C.

2.2. Receiver and optical field

We assumed a superficial tubular receiver, served by a radially staggered, surround heliostat field, comprising of 115 m^2 Sener heliostats, similar to those used at the GemaSolar plant in Spain. Heliostat reflectivity is taken as 94% [26], whilst a fouling factor of 95% [27] and heliostat availability of 99% [27] was adopted for this study. A constant extinction coefficient of 1.28 × 10^{-4} m^{-1} was adopted, as it falls about midway in the range of clear sky data reported by Ref. [28]. Guttman [29] recorded day to day differences of ±30% in the value of the extinction coefficient at White Sands, New Mexico, USA. The incident heat flux at the receiver was calculated using SolarPILOT [30], whilst the maximum receiver heat flux was limited to 1.1 MW/m^2 [27]. An energy balance for the receiver yields

$$\eta_{rec} = \frac{\alpha Q_{in} - \varepsilon\sigma A\left(T_w^4 - T_a^4\right) - hA(T_w - T_a)}{Q_{in}} \quad (1)$$

With Q_{in} the total incident radiation, α the absorptance of the receiver (0.94), ε its emissivity (0.88) in the infrared wavelength band, A the superficial receiver area, σ the Stefan-Boltzman constant, T_w the mean outer wall temperature of the receiver tubes, h the convective heat transfer coefficient and T_a the ambient air temperature. Adopting the adiabatic temperature lapse rate near the ground [31], the air temperature at the receiver is

$$T_a = T_{a,g} - 0.00975H_t \quad (2)$$

with H_t the effective tower height, measured mid-receiver. According to Young and Ullrich [32], the convection coefficient for mixed forced and free convection across a short vertical cylinder at low wind speeds, is

$$\frac{Nu_D}{\sqrt{Re_D}} = 25\sqrt{(L/D)^4 Re_D^2/Gr_L} \quad (3)$$

With D and L the receiver diameter and height respectively, and Gr, Nu and Re the Grasshof, Nusselt and Reynolds numbers. The subscript indicates the appropriate characteristic length. We have adopted the one seventh power law to estimate the wind speed at receiver height

$$\frac{V}{V_{ref}} = \left(\frac{H_t}{H_{ref}}\right)^{1/7} \quad (4)$$

The reference wind speed is measured at H_{ref}, 10 m above ground level.

It would appear that visual impact, rather than tower cost or optical efficiency is the most important consideration determining tower height, as there is no clear correlation between tower height and plant output for existing central receiver plants (Ashalim, 250 m, 110 MW_e; Crescent Dunes, 160 m, 110 MW_e; GemaSolar, 140 m, 20 MW_e; Ivanpah, 140 m, 130 MW_e; Khi Solar-1, 200 m, 50 MW_e). A tower height of 200 m was adopted for this study, at the low end of the range considered by Ref. [6] for the visual impact study.

2.3. Power block

The power block is loosely based on the Siemens SST 800 series turbine with reheat, assuming live steam pressure and temperature of 16 MPa and 540 °C respectively. We assumed three feed-water heaters with equal temperature rise over each heater. The high pressure feed-heater is fed from steam at the high pressure casing outlet, the open feed-heater (de-aerator) from the intermediate casing outlet, and the low pressure feed-heater from an extraction point in the low pressure turbine, as shown in Fig. 2. The isentropic efficiency of the high and low pressure turbines are both 85% [33] (Siemens, 2012).

The pinch point (temperature difference between salt and steam temperatures at the evaporator section inlet of the steam generator) was constrained to $\Delta T \geq 5$ °C [34].

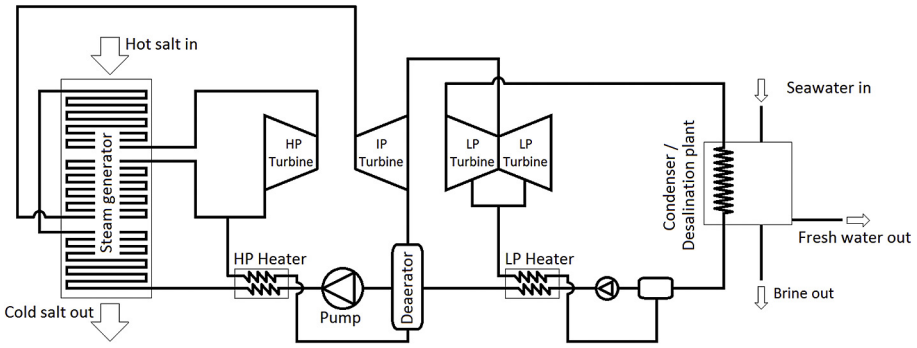

Fig. 2. Conceptual lay-out of combined power and desalination plant.

When coupled to a multi-effect distillation plant, the condenser temperature was set 4 °C above the top brine temperature [35], the latter being a parameter of the solution. A higher brine temperature will lead to an increased distillate yield and a reduced electricity output, and vice versa. For the reference case (CSP plant with direct air-cooled condenser), we have assumed a condensing temperature 25 °C above the ambient air temperature [36].

2.4. Desalination plant

Our desalination technology of choice is a multi-effect feed forward distillation plant, as the lower top brine temperature will allow lower condensing temperatures for the Rankine cycle and a better thermal to electric energy conversion. The number of effects is a parameter of the solution. A higher number of effects will increase distillate yield at an increased initial capital lay-out. Furthermore, the vertical stacked configuration as shown in Fig. 3 offers stable operation between 40 and 120% of its design rating, making it eminently suitable for solar applications [37].

We followed the modelling approach of Mistry et al. [38], but developed our own model in Microsoft Excel, using an add-in for the properties of saline water developed by Sharqawy et al. [39] and refined by Nayar et al. [40]. We adopted a modular method in which each effect and/or its subcomponents is modeled independently. Effects and/or components are coupled by mass and energy balances.

Seawater enters the first effect as a sub-cooled liquid at a pressure below the ambient pressure. A vacuum pump at the last effect controls the pressure and flow rates through each effect. The seawater is first heated to its boiling point by exhaust steam from the Rankine cycle, whilst some seawater also evaporates. The boiling point of seawater is lower than the top brine temperature by the boiling point elevation, that is a function of pressure and salinity. In the process, the steam condenses and condensate is returned to the steam generator. Distillate vapour is used to preheat whole seawater flowing towards the first effect. Brine and distillate vapour is passed on to the second effect.

Energy balance for the evaporator of the first effect shown in Fig. 4 gives

$$\dot{m}_s h_{si} + \dot{m}_f h_{fo} = \dot{m}_s h_{so} + \dot{m}_{bo} h_{bo} + \dot{m}_d h_{gd} \tag{5}$$

Water mass balance

$$\dot{m}_f = \dot{m}_{bo} + \dot{m}_d \tag{6}$$

and assuming that the distillate is pure water, a salt balance yields

$$\dot{m}_f X_f = \dot{m}_{bo} X_{bo} \tag{7}$$

For the preheater, find

$$\dot{m}_f h_{fi} + \dot{m}_d h_{gd} = \dot{m}_f h_{fo} + \dot{m}_d h_{do} \tag{8}$$

Since some distillate is condensing in the preheater, the heat transfer is expressed as

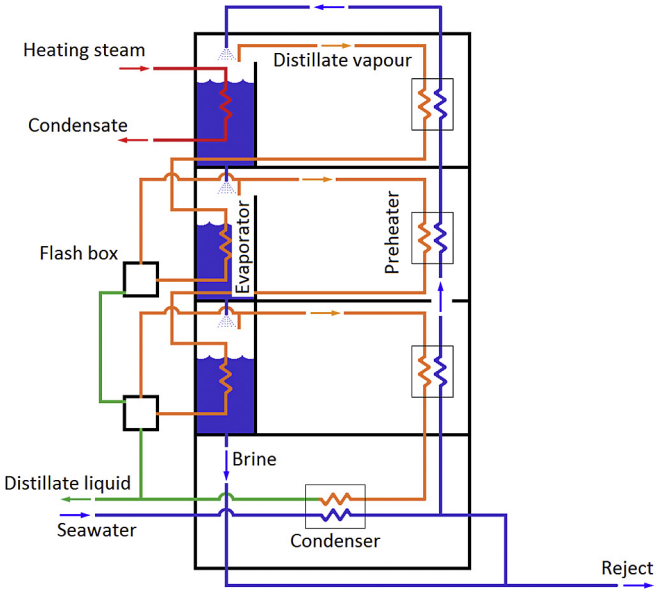

Fig. 3. Conceptual lay-out of a multi-effect stacked distillation plant.

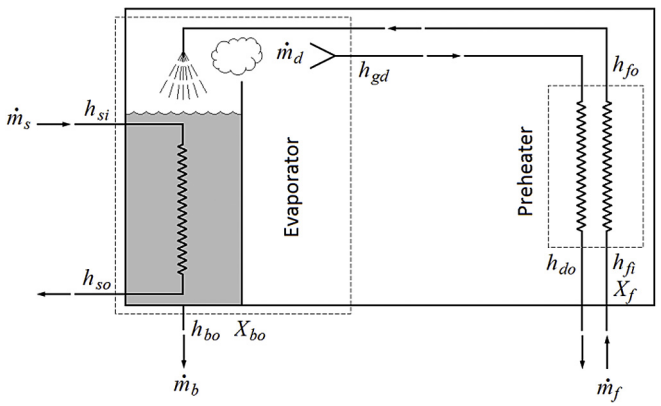

Fig. 4. Definition sketch for heat and mass transfer processes in the first effect.

$$Q_{ph} = \dot{m}_f C_{pf} \varepsilon \left(T_d - T_{fi}\right) \tag{9}$$

with

$$\varepsilon = 1 - exp(-NTU) \tag{10}$$

and

$$NTU = \frac{U_{ph} A_{ph}}{\dot{m}_f C_{pf}} \tag{11}$$

It is assumed that the heat transfer surface areas for all preheaters are identical [41]. The distillate temperature is lower than the top brine temperature by the boiling point elevation.

Some brine entering the second effect (the control volume for second effect is shown in Fig. 5) will flash over to steam due to the pressure in the second effect being lower than that in the first effect. An energy balance for the flashing process gives

$$\dot{m}_{bi} h_{bi} = \dot{m}_{be} h_{be} + \dot{m}_{d,f} h_{gd} \tag{12}$$

and a salt balance gives

$$\dot{m}_{bi} X_{bi} = \dot{m}_{be} X_{be} \tag{13}$$

whilst a water balance gives

$$\dot{m}_{bi} = \dot{m}_{be} + \dot{m}_{d,f} \tag{14}$$

Distillate vapour from the first effect is used to boil off some more vapour in the second effect. In the process, the distallate vapour is condensed. Brine, and separate streams of liquid and vapour distillate is passed on to the next effect, where the process is repeated. The salinity of the brine increases as it progresses from one effect to the next. From an energy balance over the second effect evaporator, find

$$\dot{m}_d h_{di} + \dot{m}_{be} h_{be} = \dot{m}_d h_{do} + \dot{m}_{bo} h_{bo} + \dot{m}_{d,b} h_{gd} \tag{15}$$

whilst water and salt balances give

$$\dot{m}_{be} = \dot{m}_{bo} + \dot{m}_{d,b} \tag{16}$$

and

$$\dot{m}_{be} X_{be} = \dot{m}_{bo} X_{bo} \tag{17}$$

respectively.

Since distillate is condensing, and brine boiling in the evaporator, the heat transfer for the evaporator is given by

$$Q_e = U_e A_e (T_d - T_b) \tag{18}$$

The evaporator surface area A_e is constant for all effects. U_e is the overall heat transfer coefficient for the evaporator.

Heat exchangers were not modeled in detail. Heat transfer surfaces were matched to their required duty via temperature dependent overall heat transfer coefficients proposed by El-Dessouky and Ettouny [14] specifically for desalination plant. The temperature was assumed to be the effect temperature.

Spend distillate from the first effect is send to the second effect flash box, where its pressure is lowered to that of the second effect. Consequently, some of the liquid distillate will flash back to the vapour phase. From an energy balance, find

$$\dot{m}_{d,b} h_{do} = \dot{m}_{dl} h_f + \dot{m}_{dv} h_{gd} \tag{19}$$

with h_f and h_{gd} the enthalpies of saturated liquid and vapour at the effect temperature, whilst a mass balance gives

$$\dot{m}_{d,b} = \dot{m}_{dl} + \dot{m}_{dv} \tag{20}$$

The distillate liquid is passed on to the third effect flash box, whilst the vapour is combined with the vapour that resulted from flashing and boiling in the effect to preheat the feedwater. An energy balance for the preheater yields

$$\left(\dot{m}_{d,f} + \dot{m}_{d,b} + \dot{m}_{dv}\right) h_{gd} + \dot{m}_f h_{fi} = \dot{m}_e h_{de} + \dot{m}_f h_{fo} \tag{21}$$

All the distillate produced in the last effect is condensed by the incoming seawater as shown in Fig. 6. Excess seawater is mixed with brine, and returned to the sea, whilst the remainder is passed

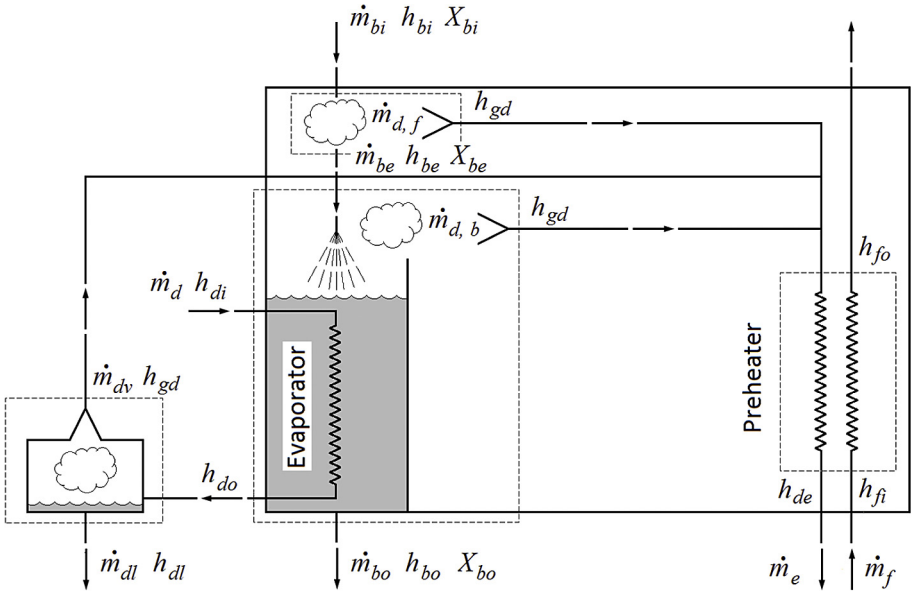

Fig. 5. Definition sketch for the heat and mass transfer processes in the second effect.

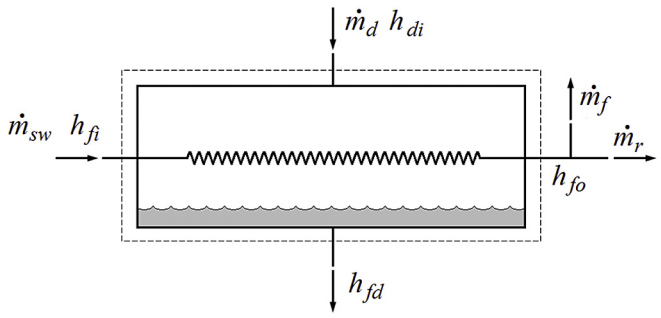

Fig. 6. Control volume for down-condenser.

on to the preheater of the last effect. The amount of reject decreases sharply with an increase in top brine temperature.

An energy balance for the condenser yields

$$\dot{m}_{sw}h_{fi} + \dot{m}_d h_{di} = \dot{m}_{sw}h_{fo} + \dot{m}_d h_{fd} \tag{22}$$

We have adopted a constant temperature rise of 15 °C for the feed-water over the condenser. The maximum salinity of brine that may be returned to the ocean is restricted, allowing us to find the feed-water flow as a function of the distillate production:

$$\dot{m}_f = \dot{m}_d + \dot{m}_b \tag{23}$$

and

$$\dot{m}_f X_{sw} = \dot{m}_b X_{max} \tag{24}$$

The excess seawater

$$\dot{m}_r = \dot{m}_{sw} - \dot{m}_f \tag{25}$$

is returned to the ocean.

A viable option would be to blend brine and excess seawater in order to relax the maximum salinity from the rather strict conditions imposed by nature conservation to a maximum prescribed by plant operation and materials.

The most probable extraction point for fresh seawater will be at Swakopmund, and in our model, we opted for an intake bay, water pre-treatment plant and a grid-powered pumping station on the coast. Seawater is pumped inland to supply the distillation plant that doubles up as a condenser for the concentrated solar power plant. An annual average water temperature of 15 °C off the Namibian coast was adopted for this study. Variations of up to 5 °C in temperature were recorded, as land winds push the cold Benguella current off-shore in summer, allowing the water temperature near the coast to increase. Due to severe erosion/corrosion expected on the coast, we anticipated that the pipeline from the coast to Arandis will be buried. As a result, seawater will reach the distillation plant without any significant temperature change. Pipe size was selected based on an optimum pipe size for chemical process plants [42].

2.5. Methodology

No long term solar irradiation data is available for Arandis, and we had to resort to solar data for the twelve month period from 1 November 2014 to 31 October 2015. We assumed that the optical field and receiver will operate through successive hourly steady states as the solar input varies. The steam generator extracts energy from the hot salt tank, and there is no direct feed from the receiver. Our operating philosophy is to run the Rankine cycle and distillation plant at full load as long as there is enough stored energy in the hot salt tank to ensure operation through the next hour. If not, the entire operation shuts down. The plant will restart once sufficient thermal energy is accumulated in the hot salt tank to ensure that the plant can run through the next hour. We assumed that start-up time from a hot start is insignificantly shorter than 1 h. This simplified operating philosophy is consistent with the anticipated flat feed-in tariff for renewable energy [7].

The plant was optimized [43] at the nominal design conditions (solar noon on autumn equinox in the Southern Hemisphere) by doing a parametric study on the variables listed in Table 1 through the ranges listed in the same table.

Operating experience and techno-economic studies from the literature indicate the distillation plants are subject to numerous constraints. Constraints adopted for this study are listed in Table 2.

In this study, we have adopted a maximum salinity of 60 g/kg, a bottom brine temperature of 40 °C, a terminal temperature difference of 4 °C at the first effect, and a temperature difference as close as possible to 2 °C between effects. The preheater terminal temperature difference was treated as a constraint.

2.6. Costing model

The proposed concentrated solar power and distillation plant at Arandis would be a first of its kind for Namibia, and no reliable costing figures are available. Our model assumes that plant components and skilled labour are imported, and international United States Dollar rates apply. The close proximity of a harbour at Walvis Bay, and the good road and rail infrastructure serving the local mining industry would soften the effect of transport cost. Furthermore, we have adopted the role of an independent power producer totally reliant on external source for the financing of the project. The duration of the loan is 20 years, and we have assumed a payment and interest holiday during the construction phase. Local tax (15% value added tax) structures, exchange rates (N$ 12.5 ≡ 1 US$), inflation (6%) and interest rates (18%) were adopted. Concentrated solar power projects are still considered a risky investment by most financiers, hence the high interest rate. Land prices in the Erongo region varies from around US$ 200 per acre for large stock farms to upwards of US$ 2000 per acre for smaller lifestyle properties; we have adopted a value of US$ 1000 per acre for this study.

Component costs for the solar-thermal plant were derived from Dieckmann et al. [45]. The large scale roll-out of solar-thermal power anticipated earlier has not materialized, with new projects skewed towards photovoltaics world-wide. Although component costs were reduced somewhat, Dieckmann et al.'s component costs remain relevant, albeit somewhat conservative. Consequently, we made no effort to take scaling and learning effects into account. Individual component costs for the solar-thermal plant are listed in Table 3.

A flat feed-in tariff of ND 1.92/kWh$_e$ [7] for electricity, and ND 45/m^3 for water [4], were adopted. It was assumed that electricity to power pumps for the distillation and reverse osmosis units on the coast can be purchased from the grid operator at the same price. Specific power consumption for the distillation plant was

Table 1
Plant design parameters for electricity/desalinated water co-generation plant.

Variable	Min	Max	Step
Solar multiple	1	4	0.2
Thermal energy storage	0	24	0.5
Top brine temperature	55	85	7.5

Table 2
Design constraints for distillation plant.

Constraint	Value	Ref
Maximum salinity of brine	≤60 g/kg	[35]
Minimum brine temperature	≥40 °C	[38]
Terminal temperature difference (1st effect)	≥2.5 °C	[35]
Terminal temperature difference (preheaters)	≥5 °C	[38]
Minimum temperature difference between effects	≥1.5 °C	[44]

Table 3
Central receiver plant component cost from Dieckmann et al. [45].

Component	Unit cost
Land	US$ 0.24/m^2
Land preparation	US$ 16/m^2
Heliostats	US$ 143/m^2
Tower	US$ 90 000/m
Receiver	US$ = 125/kW$_t$
Thermal energy storage	US$ 26/kWh$_t$
Power block	US$ 1270/kW$_e$
ACC [46]	US$ 95/kW$_e$
Contingency	19%
EPC cost	15%

added to the parasitic power consumption of the central receiver plant.

The distillation plant comprises of a pumping station and seawater inlet on the coast, connected by a pipeline to the central receiver plant. Brine and reject seawater is returned to the ocean via another pipeline to the coast. It is assumed that the return line is gravity fed, as the available pressure head due to elevation exceeds the friction losses by a factor of 25. We have ignored minor losses in both lines. The installation cost of the pipeline is estimated at ND 3 000 000/ km [47].

The desalination plant replaces the air cooled condenser in the central receiver plant. Hence, the air cooled condenser, and its parasitic power consumption (2% off gross generation) is removed from the central receiver plant. With the distillation plant an integral part of the central receiver plant, the specific power consumption of the distillation plant of 1.5 kWh$_e$/m^3 [22] was added to the parasitic power consumption of the central receiver plant.

Component costs of the distillation plant in the Middle East region were taken from Loutatidou and Arafat [48] and were applied unmodified to the Namibian scenario. However, contingency and engineering procurement and design (EPD) costs were aligned with those for the central receiver plant. A summary of component costs for the distillation plant are given are given in Table 4.

3. Results and discussion

Dall [43] found the lowest levelized cost of electricity is realized for a 100 MW$_e$ gross stand-alone solar thermal power plant at Arandis with a solar multiple of 3.3, and 13.5 h thermal energy storage. In this study, the solar thermal power plant was upgraded to 100 MW$_e$ nett at the design conditions. We have retained the solar multiple and thermal energy storage from Dall's earlier study. We deviated from Dall's original work in that the same live steam mass flow rate, temperature and pressure were used for the stand alone solar thermal plant, as well as all the cogeneration case studies.

All results are based on a terminal temperature difference of 4 °C at the first effect, a bottom brine temperature of 40 °C and a temperature difference between effects close to 2 °C:

Table 4
Distillation plant component costs from Loutatidou and Arafat [48] unless indicated differently.

Component	Unit Cost
Land (on the coast)	US$ 1000/ha
Civils (on the coast)	US$ 15/m^2
Distillation plant	US$ 1394/m^3/day
Water pre-treatment plant	US$ 55/m^3/day
Seawater intake	US$ 217/m^3/day
Pumping station[a] [17]	US$ 900/m^3/s
Pipeline [47]	ND 3,000,000/km
Contingency	7%
EPD	11%
Tax	15%
Operation and maintenance	US$ 0.125/m^3/year
Pumping cost	ND 1.9/kWh$_e$

[a] In Servert et al.'s case study, seawater is pumped 100 km inland to an elevation of 2200 m above sea level, substantially higher than the 580 m required in this study. Several pumping substations were required. Adopting their capital cost for the pumping station would lead to a conservative result.

$$\Delta T_{eff} = \frac{Top\ brine\ temp - Bottom\ brine\ temp}{N-1} \approx 2°C$$

with N the number of effects. Current results are generally more conservative than those of [43] (see Fig. 6).

The overall contribution of the distillation plant to the overall plant investment (excluding engineering, procurement and design cost, taxes and contingencies) cost is modest at 13.6%, as shown in Fig. 7. Its effect on the overall business case for a cogeneration plant is disproportionately large, as shown in Table 5. At a share of 42% of total capital investment cost, the heliostat field is the major contributor to the overall plant cost.

A direct comparison between the levelized costs of water and electricity is meaningless. Case studies were compared on the profit it can potentially generate for the plant owner, as shown in Table 5. Dieckmann et al. [45] included a profit margin for the concentrating solar power plant in contigengies, and one would expect the results to be somewhat biased. We have compared our results with the existing Trekkopje reverse osmosis plant at Swakopmund. Also shown are the results for a direct dry-cooled concentrated solar power plant. The latter two would presumably belong to different plant owners.

Financing cost in Table 5 includes debt servicing and capital repayment. It is responsible for more than 75% of the annual disbursements. Pumping cost is the other major expense, at almost 18% of annual disbursements. It is almost four times higher than the pumping cost for a reverse osmosis plant on the coast. For the

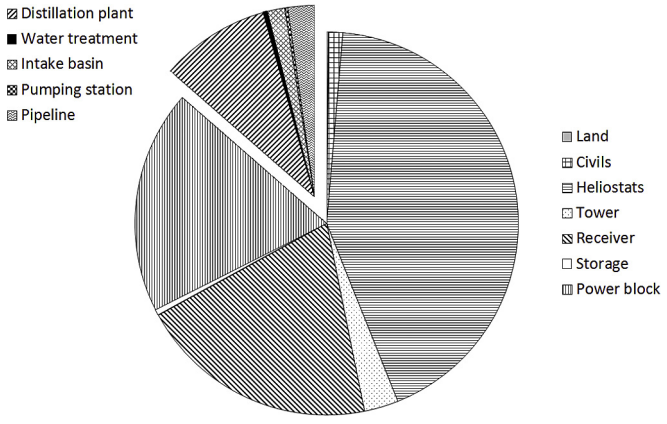

Fig. 7. Relative contribution of plant components to total investment cost.

Table 5
Main findings from simulation results.

	CSP, Dry Cooled	CSP + Multi-effect distillation Plant				RO Plant (Coast)
		$T_s = 60$ °C	$T_s = 65$ °C	$T_s = 70$ °C	$T_s = 75$ °C	
Electricity generated (GWh)	789.465	766.356	753.721	741.191	728.845	–
Financing cost (million US $)	111.137	109.517	109.513	109.430	109.425	–
Ops & maintenance (million US $)	7.000	7.000	7.000	7.000	7.000	–
Feed-in tariff (US $/kWh)	0.152	0.152	0.152	0.152	0.152	–
LCOE (US $/kWh)	0.147	0.152	0.155	0.157	0.160	–
Profit: electricity (million US $)	5.563	−0.031	−1.947	−3.769	−5.641	–
Water yield (million m^3/year)	–	10.012	12.570	15.079	17.071	20.000
Financing cost (million US $)	–	8.454	10.545	12.596	14.224	17.220
Ops & Maintenance (million US $)	–	1.252	1.571	1.885	2.134	11.200
Pumping cost (million US $)	–	26.691	26.086	28.073	28.818	7.209
Water tariff (US $/$m^3$)	–	3.600	3.600	3.600	3.600	3.600
LCOW (US $/$m^3$)	–	3.635	3.039	2.822	2.646	1.783
Profit: water (million US $)	–	−0.354	7.049	11.730	16.278	36.334
Total annual profit (million US $)	5.563	−0.385	5.101	7.962	10.637	36.334

reverse osmosis plant, only distillate needs to be pumped inland. Operating and maintenance cost contributes the rest.

Fig. 8 depicts the cumulative cash flow from the different plant configurations investigated in this study in 2017 dollars. We have assumed that all surplus cash would be used to pay off the initial debt. All co-generation options result in negative cash flows for the first four to five years, and cumulative cash flow only turns positive after nine to eleven years. In contrast, grid powered reverse osmosis yield positive cash flow from year one. However, total earnings from co-generation plant start to overtake reverse osmosis from years 15 onwards. By year 19, all co-generation plants outperform reverse osmosis. Except for a co-generation plant with a 60 °C top brine temperature, they all out-perform a stand-alone, dry cooled CSP plant.

The model is quite sensitive to economic parameters, as shown in Table 6. The upper and lower water tariffs were taken from Van der Merwe et al. [4], but the 3% change in interest rate was arbitrarily assumed. Water tariff had a dramatic effect on the distillation plant, as initial profit margins were small. It is still the most significant effect influencing the reverse osmosis plant, but its effect on the percentage change in income was less dramatic, coming from a large initial baseline. Both the dry-cooled CSP plant and cogeneration plant (only numbers for plant with top brine temperature of 65 °C are shown) are very sensitive to changes in the interest rate, due to their large initial capital outlay. Due to the small up-front investment, the grid powered reverse osmosis plant is quite insensitive to interest rate fluctuations. Changing DNI data from P50 to P90 had a very small effect. Plant sensitivity to technical inputs, like the number of effects, temperature rise over effects, heat transfer surface areas, and so forth were discussed by Dall [43]. Distillate production was optimized by Dall and Hoffmann [49].

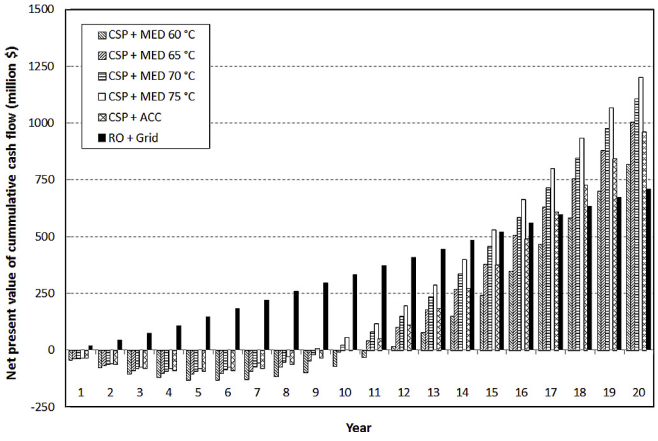

Fig. 8. Cumulative cash flows for the plant configurations investigated.

Table 6
Percentage change of different plant configurations to some input parameters.

	Water tariff (ND/m^3)			Interest rate (%)			DNI Data	
	32	45	54	15	18	21	P50	P90
Cogen	−186	–	247	473	–	−334	–	2.6
RO	−58	–	40	9	–	−9	–	–
CSP	–	–	–	182	–	−195	–	0.7

A multi-effect stacked distillation plant hooked to a 100 MW_e (net) concentrating solar thermal electricity plant is a reasonable fit to the water demand of the mines around Arandis. To match future water demand, the Rankine cycle should operate at a condenser temperature higher than 75 °C. At these temperatures, the levelized cost of electricity exceeds the proposed feed-in tariff. However, based on current water tariffs, water sales would be able to subsidize the electricity production, whilst still making a small profit overall. The unconfirmed 50% green energy credit [7] proposed by the Namibian Department of Mining and Energy was not taken into account.

Reverse osmosis is the lowest cost option for the desalination of seawater in Namibia at a levelized cost of water of about $ 1.783/m^3, compared to $ 2.646/m^3 for a multi-effect stacked distillation plant coupled to a concentrating solar thermal power plant with a condenser temperature of 75 °C. However, a cogeneration plant is financially viable, and would also address Namibia's growing demand for electricity, and at the same time, reduce the country's carbon footprint and lead to greater energy independence from its neighbours.

Pumping seawater inland is a major contributor to the levelized cost of water. Raising the seawater temperature increase over the down-condenser of the distillation plant should reduce pumping cost. However, seasonal variations of ±5 °C in water temperature off the Namibian coast would necessitate an increase in the bottom brine temperature during the summer months.

Servert et al. [17] reported that the levelized cost of water from a CSP + MED plant is about 3.6 times that of a grid-powered reverse osmosis plant for Northern Chile. In this study, the cost ratio is down to 1.48–2.04, depending on the top brine temperature. This is mainly due to the lower pumping cost, as Arandis is closer to the coast (50 km vs. 100 km), and at a significantly lower elevation

(580 m vs 2200 m above sea level). As a consequence, a CSP + MED cogeneration plant at Arandis is not only technically feasible, we found that it is also economically viable.

Moser [50] reported uncertainties of up to ± 35% in modelling output, and the figures above should be used with caution. Model sensitivity to input parameters were addressed by Dall and Hoffmann [49]. Notwithstanding, our results indicate that cogeneration of water and electricity should be an attractive option for plant owners, at least in context of the Namibian tariff structures.

Based upon the available meteorological data and our simple operating philosophy, the concentrated solar thermal power plant would not generate power for 12.6–15.2% of the year. It should be possible to make up for these shortfalls through the available hydro-electricity, as plant operators should be able to give grid controllers early warning in cases when the thermal energy storage will be depleted. However, a 100 MW_e solar thermal plant will supply about 15% of Namibia's peak demand, making a smaller plant perhaps more attractive from a grid control perspective. Scaling down the solar thermal plant would increase the levelized cost of electricity, and be incapable of meeting the fresh water demand.

4. Conclusion

Replacing the air cooled condenser on a central receiver solar thermal power plant with a low temperature multi-effect distillation plant, would reduce the plant's thermal efficiency, and drive the levelized cost of electricity above the proposed feed-in tariff for Namibia. At top brine temperatures above 65 °C, the production of distillate and selling it at the existing high water tariff is sufficient to offset the nett loss from electricity. Potable water production at these temperatures is sufficient to service the current fresh water demand from mines around Arandis. This makes cogeneration of electricity and potable water an economically viable option for a single plant owner/operator.

Pumping seawater 50 km inland is a main contributor to water cost, and at present, multi-effect distillation is not cost competitive with a reverse osmosis plant on the coast. The low solar resource on the coast does not allow for a central receiver plant closer to the coast. Assumptions in this paper are more conservative than those of Dall [43], resulting in the levelized cost of water being about $ 0.7/m^3 higher. Increasing the temperature rise over the down-condenser should reduce the reject, and hence total seawater flow, but would also result in raising the bottom brine temperature and a decrease fresh water production.

At 100 MW_e, the central receiver plant would be capable to supply 15% of Namibia's peak electricity demand. In such a scenario, the value of a central receiver plant with thermal energy storage, should make it attractive to grid controllers. The simple operating philosophy adopted in this paper assumes no interference from grid control. Choosing the optimal plant configuration that would maximize revenue for the plant owner/operator would be a compromise between the levelized cost of water and electricity, tariff structures, demand profiles and operating philosophy.

References

[1] M. Pryor, B. Blanco, Trekkoppje desalination plant, Imiesa Mag. 2010 (2010) 25–28. July.
[2] H. Reid, L. Sahlén, J. McGregor, J. Stage, The economic impact of climate change in Namibia: how climate change will affect the contribution of Namibia's natural resources to its economy, in: Environmental Economics Programme Discussion Paper 07–02, November 2007, 2007.
[3] Central Intelligence Agency, The World Factbook 2013-14, 2013. Washington.
[4] A. Van der Merwe, et al., Social and Environmental Impact Assessment for the Proposed Rössing Uranium Desalination Plant Near Swakopmund, Namibia, 2015. Aurecon Report no. 9408/110914, January 2015.
[5] M. Rämä, E. Pursiheimo, T. Lindroos, K. Koponen, Development of Namibian Energy Sector, 2013. VTT Technical Research Centre of Finland Report VTT-R-07599-13.
[6] F. Gresse, S. Clark, Amended Environmental and Socio-economic Impact Assessment for a Concentrated Solar Plant Facility Near Arandis in the Erongo Region – Draft Amendment Report, 2016. Aurecon Namibia Report No. 10816.
[7] Anonymous, National Renewable Energy Policy for Namibia, Electricity Control Board Draft Policy Document, June 2016, 2016.
[8] Z. Viranyi, NamPower 2015 Annual Report, NamPower, Windhoek, 2015.
[9] J.L. Sawin, K. Seyboth, F. Sverrisson, E. Martinot, Renewables 2016: global status report, in: Renewable Energy Policy Network for the 21st Century, Paris, 2016.
[10] Anonymous, Vision 2030, National Planning Commission of Namibia, 2008. http://www.npc.gov.na.
[11] S.A. Kalogirou, Seawater desalination using renewable energy sources, Prog. Energy Combust. Sci. 31 (3) (2005) 242–281.
[12] L.F. Greenlee, et al., Reverse osmosis desalination: water sources, technology, and today's challenges, Water Res. 43 (9) (2009) 2317–2348.
[13] M. Isaka, Water desalination using renewable energy, in: IEA-ETSAP and IRENA Technology Policy Brief I12 – January 2013, 2013.
[14] H.T. El-Dessouky, H.M. Ettouney, Fundamentals of Salt Water Desalination, second ed., Elsevier, Amsterdam, 2002.
[15] A. Al-Karaghouli, L.L. Kazmerski, Energy consumption and water production cost of conventional and renewable-energy-powered desalination processes, Renew. Sustain. Energy Rev. 24 (2013) 343–356.
[16] S.A. Kalogirou, Survey of solar desalination systems and system selection, Energy 22 (1997) 69–81.
[17] J.F. Servert, E. Cerrajero, E.L. Fuentealba, Synergies of solar energy use in the desalination of seawater: a case study in northern synergies of solar energy use in the desalination of Seawater: a case study in northern Chile, in: AIP Conference Proceedings 1734 (SolarPACES 2015), 140002, 2016.
[18] F. Trieb, Concentrating solar power for seawater desalination, German aerospace center (DLR), in: Institute of Technical Thermodynamics Report, November 2007, 2007.
[19] C.N. Papanicolas, et al., CSP cogeneration of electricity and desalinated water at the Pentakomo field facility, in: AIP Conference Proceedings 1734 (SolarPaces 2015), 100008, 2016.
[20] A. Ghobeity, et al., Optimal time-invariant operation of a power and water cogeneration solar-thermal plant, Sol. Energy 85 (9) (2011) 2295–2320.
[21] M. Moser, F. Trieb, T. Fichter, Potential of concentrating solar power plants for the combined production of water and electricity in MENA Countries, J. Sustain. Dev. Energy Water Environ. Syst. 1 (2) (2013) 122–141.
[22] P. Palenzuela, et al., Comparison between CSP+MED and CSP+RO in Mediterranean area and MENA region: techno-economic analysis, Energy Procedia 69 (2015) 1938–1947.
[23] C. Frantz, B. Seifert, Thermal analysis of a multi effect distillation plant powered by a solar tower plant, Energy Procedia 69 (2015) 1928–1937.
[24] Anonymous, (s.a.), NamPower, http://www.nampower.com.na.
[25] Namibia Energy Institute, Pre-feasibility Study for the Establishment of a Pre-commercial Concentrated Solar Power Plant in Namibia, 2012. Namibia University of Science and Technology Report, http://nei.nust.na/sites/default/files/projects/NA.2012.R.005.2.pdf. (Accessed 29 July 2017).
[26] F. Tellez, et al., State of the Art in Heliostats and Definition of Specifications: Survey for a Low Cost Heliostat Development, 2014. STAGE-STE Project Report.
[27] C.S. Turchi, G.A. Heath, Molten Salt Power Tower Cost Model for the System Advisor Model (SAM), 2013. National Renewable Energy Laboratory Technical Report NREL/TP-5500-57625.
[28] N. Hanrieder, et al., Atmospheric extinction/attenuation in simulation tools for solar tower plants, in: SolarPACES 2016, 2016.
[29] A. Guttmann, Extinction Coefficient Measurements on Clear Atmospheres and Thin Cirrus Clouds, 1968. General Electric Company, Missile and Space Division Report 68SD1516.
[30] M.J. Wagner, SolarPILOT Users Manual, 2015.
[31] D.G. Kröger, Air-cooled Heat Exchangers and Cooling Towers, Penwell Books, 2004.
[32] M.F. Young, T.R. Ulrich, Mixed convection heat transfer from a vertical heated cylinder in a crossflow, Int. J. Heat Mass Transf. 26 (12) (1983) 1889–1892.
[33] SIEMENS energy, (s.a.), http://www.energy.siemens.com/hq/pool/hq/power-generation/steam-turbines/sst-800/Brochure-Siemens-SST-800_ Steam-Turbine_Interactive.pdf.
[34] A. Behbahani-nia, S. Sayadi, M. Soleymani, Thermo-economic optimization of the pinch point and gas-side velocity in heat recovery steam generators, J. Power Energy 224 (6) (2010) 761–771.
[35] J. Gebel, Chapter 2. Thermal desalination processes, in: J. Kucera (Ed.), Desalination: Water from Water, first ed., Wiley, 2014.
[36] J.P. Pretorius, A.F. Du Preez, Eskom cooling technologies, in: Proceedings of the 14th IAHR Conference, Stellenbosch, 2009.
[37] A.M. El-Nashar, A. Qamiyeh, Simulation of the performance of MES evaporators under unsteady state operating conditions, Desalination 79 (1990) 65–83.
[38] K.H. Mistry, M.A. Antar, J.H. Lienhard, An improved model for multiple effect distillation, Desalination water Treat. 51 (4) (2012) 1–15.
[39] M.H. Sharqawy, J.H. Lienhard, S.M. Zubair, Thermophysical properties of seawater: a review of existing correlations and data, Desalination Water Treat.

16 (2010) 354–380.
[40] K.G. Nayar, M.H. Sharqawy, L.D. Banchik, J.H. Lienhard, Thermophysical properties of seawater: a review and new correlations that include pressure dependence, Desalination 390 (2016) 1–24.
[41] H.T. El-Dessouky, H.M. Ettouney, Multiple-effect evapo-ration desalination systems: thermal analysis, Desalination 125 (1999) 259–276.
[42] M.S. Peters, K.D. Timmerhaus, Plant Design and Economics for Chemical Engineers, fourth ed., McGraw-Hill, 1991.
[43] E.P. Dall, Integrating Desalination with Concentrating Solar Power: Large Scale Cogeneration of Water and Electricity (M. Eng. Thesis), Stellenbosch University, 2017.
[44] A. Ophir, F. Lokiec, Review of MED fundamentals and costing, in: International Conference on Desalination Costing, Limassol, Cyprus, 2004.
[45] S. Dieckmann, et al., LCOE reduction potential of parabolic trough and solar tower CSP technology until 2025, in: SolarPACES 2016, Abu Dhabi, 2016.
[46] J.S. Maulbetch, M.N. DiFilippo, Cost and Value of Water Use at Combined-cycle Power Plants, 2006. California Energy Commission Report CEC-500-2006-034.
[47] NamWater, (2016), http://www.namwater.com.na/index.php?option= com_content&view=article&layout=edit&id=65 (Accessed 2 March 2016).
[48] S. Loutatidou, H.A. Arafat, Techno-economic analysis of MED and RO desalination powered by low-enthalpy geothermal energy, Desalination 365 (2015) 277–292.
[49] E.P. Dall, J.E. Hoffmann, The techno-economic optimization of a 100MWe CSP-desalination plant in Arandis, Namibia, in: AIP Conference Proceedings 1850 (SolarPaces 2016), 170002, 2017.
[50] M. Moser, Combined Electricity and Water Production Based on Solar Energy (PhD Thesis), University of Stuttgart, 2014.